





Article

Facilitating the Transition to an Inverter Dominated Power System: Experimental Evaluation of a Non-Intrusive Add-On Predictive Controller

Mazheruddin H. Syed ^{1,*}, Efren Guillo-Sansano ¹, Ali Mehrizi-Sani ² and Graeme M. Burt ¹

¹ Institute for Energy and Environment, University of Strathclyde, Glasgow G1 1RD, UK; efren.guillo-sansano@strath.ac.uk (E.G.S.); graeme.burt@strath.ac.uk (G.M.B.)

² Bradley Department of Electrical and Computer Engineering, Virginia Tech, Blacksburg, VA 24601, USA; mehrizi@vt.edu

* Correspondence: mazheruddin.syed@strath.ac.uk

Received: 2 July 2020; Accepted: 12 August 2020; Published: 16 August 2020



Abstract: The transition to an inverter-dominated power system is expected with the large-scale integration of distributed energy resources (DER). To improve the dynamic response of DERs already installed within such a system, a non-intrusive add-on controller referred to as SPAACE (set point automatic adjustment with correction enabled), has been proposed in the literature. Extensive simulation-based analysis and supporting mathematical foundations have helped establish its theoretical prevalence. This paper establishes the practical real-world relevance of SPAACE via a rigorous performance evaluation utilizing a high fidelity hardware-in-the-loop systems test bed. A comprehensive methodological approach to the evaluation with several practical measures has been undertaken and the performance of SPAACE subject to representative scenarios assessed. With the evaluation undertaken, the fundamental hypothesis of SPAACE for real-world applications has been proven, i.e., improvements in dynamic performance can be achieved without access to the internal controller. Furthermore, based on the quantitative analysis, observations, and recommendations are reported. These provide guidance for future potential users of the approach in their efforts to accelerate the transition to an inverter-dominated power system.

Keywords: control; inverters; inverter-dominated grids; power system transients; predictive control

1. Introduction

The integration of renewables within the electrical power system is a trend encouraged in many countries driven by environmental policies, fossil fuel restrictions, and energy security requirements. US Energy Information Administration projects that renewables (e.g., solar, wind, and hydro) will provide nearly half (49%) of the world's electricity demand by 2050 as end-use consumption experiences increasing electrification. For comparison, in 2018, only 28% of global electricity was generated from renewable energy sources, more than half of which was from hydropower.

In particular, both the United States and United Kingdom have increasingly installed more renewables over the past few years. In the United States, electricity generation from solar and wind resources has been steadily increasing since 2013. Wind and solar accounted for 6.8% and 2.8% of the total electricity generation in September 2019, a 31% and 15% increase from the same period in 2018 (while the total energy production increased by a mere 0.9%). Similarly in the United Kingdom, the share of generation from renewables grew to 38.9% in the third quarter of 2019, marginally exceeding generation from gas for the first time. On- and offshore wind dominated the renewables share at 19% with biomass second at 12%.

The increasing incorporation of power electronically interfaced renewables is accelerating the paradigm shift from a traditional synchronous generation dominated power system to an inverter-dominated power system. In a renewables-rich inverter-dominated grid, the operation and control under low and variable inertia conditions need renewed attention for the following reasons. First, lower inertia corresponds to a larger deviation of the system variables from their reference set points for any given system disturbance. Moreover, some disturbances may cause enough deviation to lead to instability. Second, the inverters themselves, due to their semiconductor switches, are more sensitive to such deviations which may cause physical damage. Third, the expected diurnal changes in the generation-load patterns can require frequent retuning of the controllers.

Several efforts have attempted to design robust set point tracking controllers to accommodate such emergent requirements. The established approaches in the literature, as summarized in Table 1, require either the system model or access to the internal parameters of the controller. These requirements present limitations due to vendor practices that do not always provide access to the internal parameters of the inverter and the unavailability of the system model with inverters. These approaches are often decentralized, implemented within an inverter, to ensure fast and high precision set point tracking—yielding a dynamically robust performance. The response of more than one inverter can be coordinated to support the response of a particular individual inverter or to achieve a global common objective. Such approaches, referred to as distributed control approaches, have been abundantly proposed in the literature [1–4]. However, the focus of this paper is on decentralized approaches to improve the dynamic response of inverters.

Table 1. Comparison of methods to improve the dynamic response of a system

Approach	References	No Model	Noninternal
PI gain scaling	[5,6]	✓	X
Set point ramping		✓	✓
Model predictive control	[7–11]	X	X
Adding a D-term to PI	[12–14]	X	X
Extremum seeking	[15–22]	✓	X
Posicast	[23–28]	X	✓
Sliding mode control	[29–32]	X	X
Model free control	[33–38]	✓	X

It is also important to note that the control approaches summarized in Table 1 are mutually exclusive, i.e., only one chosen approach can be implemented for a given set point tracking objective. An alternative approach is to supplement the existing controllers with an add-on controller to enhance its performance under abnormal circumstances. Examples of such control approaches in the literature are adaptive gain adjustments of controllers using methods such as fuzzy logic [39–41] or more recently machine learning (also referred to as data-driven or artificial intelligence methods) [42,43]. Although such approaches are supplementary to the existing controllers, modification of the gain/parameters requires access to the internal control itself.

In [44], an add-on controller, referred to as SPAACE (set point automatic adjustment with correction enabled), that employs predictive set point modulation (SPM) to ensure robust performance subject to uncertain system conditions is proposed. SPAACE modifies the reference set point without the need for access to the low-level controller or knowledge of the system, in contrast to formerly described controls. Furthermore, SPAACE can be incorporated within any set point tracking application, independent of the primary control approach utilized (such as Proportional-Integral or model predictive control). Such an approach can be incorporated within existing devices within the field, improving their response by (i) reducing the overshoot, (ii) reducing the settling time, or (iii) both—thereby enhancing the utilization of existing infrastructure. The effectiveness of SPAACE to enhance dynamic performance of a system with (i) no access to its internal controller and (ii) minimal

system knowledge is shown in [45]. SPAACE uses prediction of the response behavior, and a number of predictors are proposed, with their applicability for varied applications demonstrated in [46–49].

Theoretically, the SPAACE approach is well-established, with extensive mathematical formulations, stability analysis, and simulation-based performance evaluation published. However, the following research gaps still exist:

- The choice of predictor for a given application has not been discussed.
- The fundamental hypothesis of SPAACE, i.e., the feasibility of its incorporation without requiring access to an internal controller, has not been verified. One reported experimental evaluation of SPAACE was limited to the implementation of SPAACE within the development environment of an inverter controller itself [45].
- SPAACE is a generic approach with wide application potential, yet its adoption and deployment are limited due to a lack of established evidence of its practical feasibility for real-world applications.

This paper addresses these three identified gaps via the following contributions:

- The practical feasibility and robustness of SPAACE have been established utilizing a high fidelity hardware-in-the-loop systems level test bed. Conventional approaches to DER validation, commonly undertaken as equipment testing [50], are unable to de-risk the performance of the control when connected to an unknown and continuously changing system. The systems level test bed, with its reproduction of close to real-world environments, enabled the rigorous validation of SPAACE, endowing high confidence in its performance.
- For the DER controller application under consideration, a comprehensive evaluation with a set of practical variations is undertaken, i.e., analysis of choice of predictors, implementations (within and outwith the DER inherent controller), expected modes of operation and subject to a selected range of day to day operational scenarios.
- The methodological approach to ascertain computational and dynamic performance, and the subsequent detailed quantitative analysis, form the basis for the observations and recommendations reported. These are intended to serve as a reference guide for potential future users of the approach.

Therefore, this paper, with its key contributions and findings, provides archived evidence of the feasibility and applicability of SPAACE for DERs, building confidence for its adoption in the real world (by distribution system operators, virtual power plant operators or demand aggregators) and thereby facilitating the transition of the power system to an inverter-dominated grid.

2. Predictive Set Point Modulation

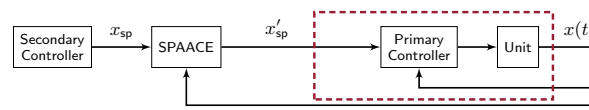
The predictive set point modulation approach, referred to as SPAACE, is a control method proposed to enhance the dynamic performance of a system with limited model information and no access to its internal controller parameters. Its incorporation enables the realization of a dynamically robust overall control architecture. In this section, the fundamentals of SPAACE are explained, including the theoretical foundation and the role of prediction strategies, and this is followed by the practicalities of parameter selection and real-world applications.

2.1. Fundamentals of Space

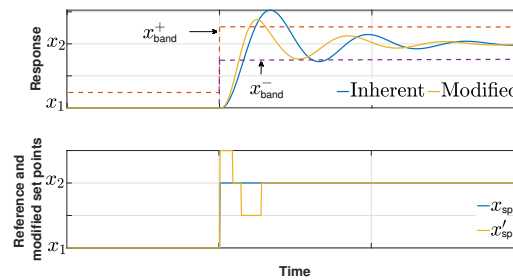
2.1.1. Theoretical Foundation

Consider a single-input single-output (SISO) unit (dashed box in Figure 1a); denoting the reference set point of this controlled unit as x_{sp} and its measured output as $x(t)$, the system representation with the incorporation of SPAACE as an add-on to the existing controllers of the unit is shown in Figure 1a. The primary controller is typically a PI-based controller designed for set point tracking; the secondary controller is a higher-level controller that decides the system reference set points. SPAACE monitors

the response $x(t)$ and based on its trend and proximity to the constraints, applies a temporary change in the reference set point $x_{sp}(t)$, denoted by x'_{sp} , to achieve the desired response trajectory.



(a) Relationship between SPAACE and existing controllers.



(b) Demonstration of SPAACE performance. Top: the response with and without SPAACE; bottom: the modified set point created by SPAACE.

Figure 1. Fundamentals of the SPAACE operation.

To explain this further, consider the example presented in Figure 1b. The original system response is referred to as the inherent response while the response with SPAACE is referred to as the modified response. For a step change in the reference set point x_{sp} from x_1 to x_2 ($x_2 > x_1$), the inherent and modified responses of the system are presented. The inherent response exhibits undesired dynamic characteristics such as large overshoot and a long settling time. Conventionally, such characteristic behavior of the controller can be alleviated by controller redesign- requiring knowledge of system parameters and access to the internal controller parameters. In contrast to the conventional approach, SPAACE responds to such a scenario by treating the original controller as a black box. As shown in Figure 1b, SPAACE defines a tolerance band around the set point and upon digression of the response outside the defined tolerance band ϵ , a modified set point x'_{sp} is issued to remedy the situation as

$$x'_{sp} = \begin{cases} x_2, & x_{\text{band}}^+ > x(t) > x_{\text{band}}^- \\ (1 - m)x_2, & x(t) > x_{\text{band}}^+ \\ (1 + m)x_2, & x(t) < x_{\text{band}}^- \end{cases} \quad (1)$$

where m is a scaling factor. By shaping the response to be limited to the band around the set point, smaller overshoot and shorter settling times are obtained represented by the modified response. A negative step change ($x_1 > x_2$) is dealt with similarly.

SPAACE does not limit itself to issuing only one temporary set point modification; if after one set point modification the response still does not follow the desired trajectory, SPAACE issues subsequent set point changes. However, SPAACE includes logic to avoid (i) issuing too many set point modifications within a short period of time which may subject the system (especially if mechanical) to stress, and (ii) applying indefinite set point modifications if for any reason they do not improve the system response.

The theoretical foundations pertaining to the existence of an improved response for several classes of dynamic systems can be found in [46–48].

2.1.2. Prediction Strategies

The operation of the SPAACE as defined in Equation (1) is responsive. The performance of SPAACE can be further improved if a preemptive operation is enabled by utilizing a predicted value of

$x(t)$, denoted by $\hat{x}(t)$ [49]. For a given response $x(t)$, the prediction method estimates the response at time T_{pred} into the future, where T_{pred} is the horizon of prediction. Any prediction method relies on n past historical data points and the number n depends on both the prediction method and the emphasis on historical data points: a smaller n produces predictions that rely only on recent past data but may suffer from noise, whereas a larger n produces smoother predictions but may slow down the response.

Each prediction method fits a parametrized function to the past measurements of the controlled variable $x(t)$ and uses this fit to estimate the future value of $x(t)$. Data fitting is performed using well-established methods such as least-square error (LSE). To ensure real-time implementation, the predictors typically employ cases of LSE that allow for significant simplifications, enabling their use for SPAACE with a smaller sampling time.

In this paper, we discuss and compare the results for three prediction methods as reported in the literature: linear, quadratic, and exponential. Other prediction methods have also been employed in SPAACE, e.g., lead compensator in [45] and Lagrangian polynomials in [47].

- (a) Linear prediction: Linear prediction, arguably the simplest predictor, uses the following fitting function:

$$\hat{x}(t_0 + T_{\text{pred}}) = x(t_0) + r(t_0)T_{\text{pred}}, \quad (2)$$

where $r(t_0)$ is the average rate of change calculated over the historical data based on LSE. With only one historical data point, linear prediction essentially results in the current value of $x(t)$ being equal to the average of the historical data point and the predicted term:

$$\hat{x}(t_0 + T_{\text{pred}}) = 2x(t_0) - x(t_0 - T_{\text{pred}}) \quad (3)$$

- (b) Quadratic prediction: In quadratic prediction, two parameters need to be calculated based on LSE:

$$\hat{x}(t_0 + T_{\text{pred}}) = x(t_0) + r(t_0)T_{\text{pred}} + \frac{1}{2}q(t_0)T_{\text{pred}}^2 \quad (4)$$

where $r(t_0)$ is as defined previously and $q(t_0)$ is a measure of the second derivative of historical data—both calculated based on the LSE formulation.

- (c) Exponential prediction: Exponential prediction assumes that in the short-term, the response of the controlled system can be approximated as an exponential rise or decay. Consequently, it fits an exponential function to the historical data as

$$\hat{x}(t + T_{\text{pred}}) = ae^{b(t_0 + T_{\text{pred}})} \quad (5)$$

where a and b are calculated based on LSE.

2.2. Implementation Considerations

2.2.1. Parameter Selection

The fundamental premise of SPAACE is to ensure that parameter selection does not represent a complex task. This is achieved through the adaptive nature of SPAACE as it continually monitors the response and its reference tracking performance. However, the discussion below offers some insights on best practices for choosing SPAACE parameters:

- (a) Scaling factor: Selecting a smaller m creates modified set points that are closer to the original set point and thus changes to the set point are smaller and smoother. In contrast, a larger m introduces more severe set point changes that can help with achieving faster damping. In most cases, a modest value of $m = 0.2$ seems to produce reasonably fast results. A more detailed discussion of the effect of m on the system performance is presented in [47,49]; an analytical discussion is presented in [46].

- (b) Prediction strategy and prediction horizon: Several parameters can affect the accuracy of the prediction. In addition to the nature of the system response which suggests the type of fitting function (prediction strategy), prediction horizon T_{pred} and window of prediction history T_{past} are important design parameters. In general, T_{pred} should correspond to the inverse of the system dominant natural frequency ω_0 . That is, a faster system needs a smaller T_{pred} and vice versa. Heuristically, an acceptable rule of thumb is to choose $T_{\text{pred}} = 10 \times 2\pi/\omega_0$.
- (c) Tolerance band: Typically the band is chosen to be symmetrical around the set point, but this is not a requirement for SPAACE operation, rather a design preference.

2.2.2. Real-World Implications

- (a) Feasibility: Most real-world systems are non-linear in nature, for which linear (taking advantage of established linearization methods) and non-linear control approaches have been widely utilized. As SPAACE is an add on controller, its incorporation is independent of the control approach (linear or non-linear) and the non-linearities within the unit under consideration. Therefore, in theory, SPAACE can be incorporated within a unit under consideration for any application where precise and high-speed set point tracking is imperative. By enabling the unit under consideration to be treated effectively as a black box, SPAACE can increase the potential utilization of the existing infrastructure by reducing transients, which in turn reduces the need to overdesign the system.

Furthermore, the stability of SPAACE was discussed in [46]. It was shown that the incorporation of SPAACE within an apparatus does not impact the stability of the wider system, i.e., if the system with the apparatus was stable without SPAACE, it will remain stable with the incorporation of SPAACE. Therefore, SPAACE can readily be adopted within power system applications, ranging from small isolated systems such as electric propulsion applications to larger systems such as HVDC segmented power systems.

This paper, in particular, discusses the incorporation of SPAACE in DERs coupled to the remainder of the power system via power electronic interfaces (inverters or converters). This choice is motivated by the current practices and challenges faced by the community: transition to a renewable rich inverter-dominated grid (utility systems), interest in incorporation within small-scale systems with variable and flexible architectures (remote microgrids and propulsion applications), to name a few. Furthermore, it provides a more relevant example for demonstration as DER manufacturer's practices historically present limitations in access to the internal parameters of the inverter and the unavailability of the system model with inverters.

- (b) Architecture and Communications: SPAACE is designed for incorporation within an individual apparatus with a view to improving its dynamic response. SPAACE does not require any additional information outwith the apparatus, and therefore no communication is required. From an architectural perspective, the implementation of SPAACE can be referred to as decentralized. Depending on whether SPAACE is incorporated within the controller of the DER or on an external controller, very short distance communications via analog connection may be present.
- (c) Responsibility: The responsibility to incorporate SPAACE would essentially lie with the owner of the DER. An end user, such as a residential customer with a battery energy storage system (BESS) interfaced via an inverter, might not have an incentive for the incorporation of SPAACE. However, the benefits the approach brings to the wider grid system might interest distribution system operators, virtual power plant operators, or demand aggregators to provide incentives to the end user for its incorporation. Alternatively, this can be set forth as a requirement by a demand aggregator for any end user BESS unit to participate within ancillary service markets.
- (d) Commercialization: The details of the implementation of SPAACE and its corresponding prediction strategies have been summarized in this work. SPAACE does not exist as a commercial product, however, the entities identified above (distribution system operators,

virtual power plant operators, or demand aggregators) can develop their own solutions with confidence instilled in real-world applicability through contributions of this paper.

3. Experimental Setup

This paper validates several variants of the SPAACE algorithm in both an experimental setup and a real-time HIL environment to determine its practicality.

3.1. Test Rig

The performance evaluation of SPAACE is undertaken at the University of Strathclyde's Dynamic Power Systems Laboratory (DPSL). DPSL Microgrid is a 115 kVA, 400 V three-phase facility; its simplified one-line diagram is shown in Figure 2a. DPSL comprises equipment representing both conventional and non-synchronous generation, static and dynamic loads, arranged in such a way as to be able to run as three independent islands (or cells, as in Figure 2a) or brought together in any combination as a single system. State-of-the-art HIL techniques such as seamless initialization and synchronization of large test setups [51], experimental setup time-delay characterization [52] and measurements delay identification [53] and compensation [54] enable the realization of a high fidelity systems-level testing facility able to robustly de-risk novel control solutions for emerging power systems.

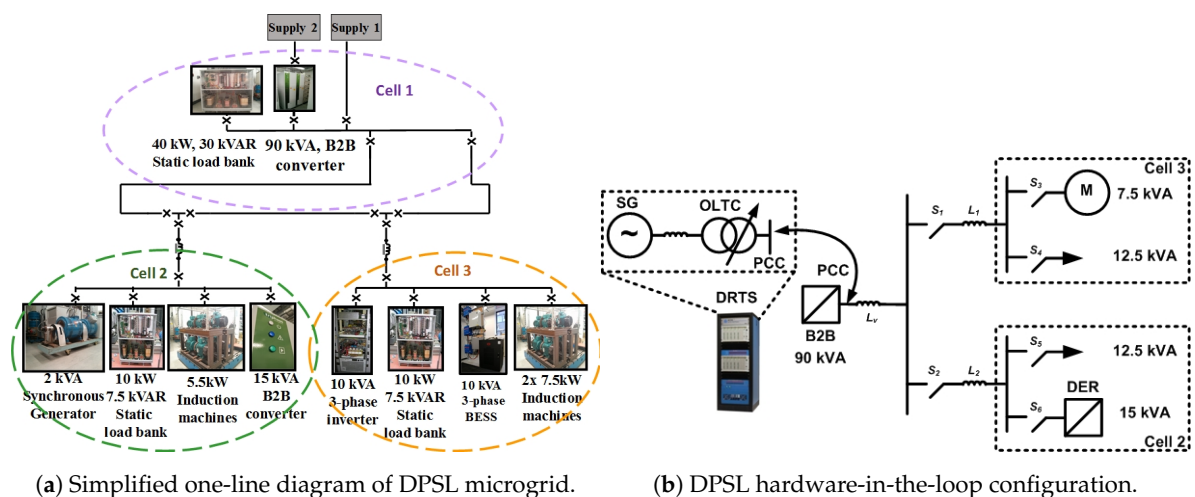


Figure 2. Test rig and hardware-in-the-loop configuration.

3.2. Test Configurations

The DPSL hardware-in-the-loop configuration utilized for the validation is presented in Figure 2b. A 15 kVA back to back (B2B) power module by Triphase is used as the DER unit, referred to as TP15 henceforth. The rest of the network constitutes a 90 kVA B2B Triphase power module serving as a grid emulator, two 12 kVA load banks, and a 7.5 kVA induction motor. A simple network, comprising a synchronous generator (SG) and an on load tap changer (OLTC) simulated within a digital real-time simulator (DRTS), provides the reference voltage for reproduction by the 90 kVA power interface. The chosen configuration is one of many configurations made possible by the flexible architecture of the DPSL Microgrid (Figure 2a). The two bus configuration is representative of a community microgrid with a lumped representation of residential customers, water pumps, and energy storage systems [55,56]. Larger system studies can be undertaken owing to the power hardware-in-the-loop capability of the DPSL, although this has not been fully exploited here. Examples of such setups for varied applications can be found in [57–60].

As SPAACE is an add-on controller, two different implementation approaches for its real-world applications are possible as described next.

3.2.1. Space within the Der Controller

If the controller of the DER is open for modifications by the user, the SPAACE algorithm can be implemented within the development environment of the DER controller. This is the most straightforward implementation of SPAACE. This implementation within the DPSL is shown in Figure 3a where the SPAACE algorithm is implemented within the controller (real-time target-RTT) of the TP15 power module.

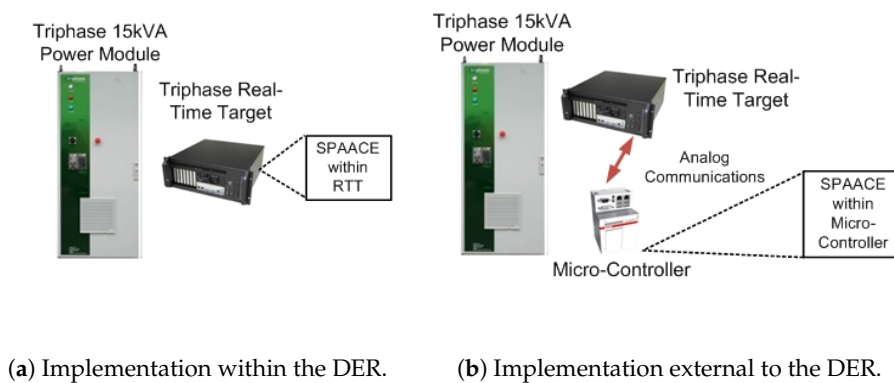


Figure 3. Network and test configurations within the DPSL.

3.2.2. Space Outwith the Der Controller

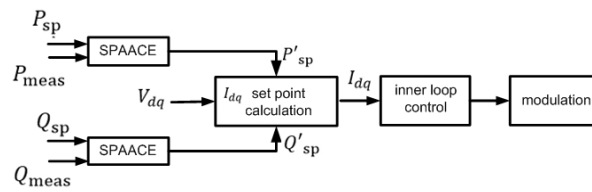
As discussed previously, SPAACE does not necessarily need access to the lower-level controls of the DER, it can be implemented within an external RTT or microcontroller. This still requires the DER to accept analog or digital communications, which most vendors provide, specifically when the development environment is closed for users. This implementation within the DPSL is shown in Figure 3b. The network configuration remains the same as explained earlier except that SPAACE is implemented within an external controller communicating with TP15 using analog communication. A twisted pair copper wire is used for the analog communications, with a propagation speed of $\sim 2 \times 10^8$ m/s and the distance between the microcontroller and TP15 of approximately 50 m, yielding a delay of approximately 2.5 μ s.

3.3. Controls for Grid-Connected and Islanded Operation

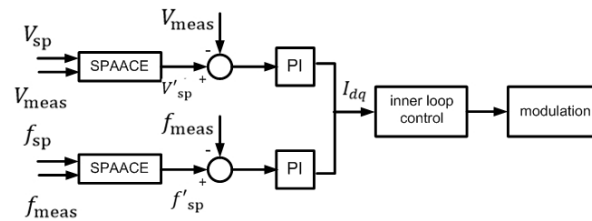
To demonstrate the applicability of SPAACE, two scenarios are considered for the operation of the DER: (i) grid-connected, and (ii) islanded. The incorporation of SPAACE in these two modes are discussed below:

3.3.1. Grid-Connected Operation

In the grid-connected mode, the DER is operated as a current-controlled voltage source. The real and reactive power set points are received by the DER controller. The incorporation of SPAACE within such DER control is shown in Figure 4a, where P_{sp} , Q_{sp} are the real and reactive power set points; P_{meas} , Q_{meas} are the measured real and reactive powers; and P'_{sp} , Q'_{sp} are the SPAACE-modified real and reactive power set points. V_{dq} is the direct and quadrature components of the voltage obtained by Park's transform. The inputs of the inner current control loop are the direct and quadrature components of the current I_{dq} ; its output is sent to the modulation block for the generation of the gating signals. SPAACE modulates the real and reactive power reference set points to improve the dynamic response.



(a) Grid connected DER control with SPAACE.



(b) Isolated DER control with SPAACE.

Figure 4. SPAACE incorporation within the DER control.

3.3.2. Isolated Operation

In the isolated mode of operation, a DER is responsible for regulating the voltage and frequency at its output terminal. A single DER responsible for maintaining the voltage and frequency of a small microgrid is considered in this paper. The incorporation of SPAACE within such DER control is shown in Figure 4b, where V_{sp} , f_{sp} are the voltage and frequency set points; V_{meas} and f_{meas} are the measured voltage and frequency; V'_{sp} , f'_{sp} are the SPAACE-modified set points of voltage and frequency.

4. Performance Evaluation

This section analyzes the performance of SPAACE. The methodology for the evaluation is presented followed by the computational and dynamic performance evaluation.

4.1. Methodology

The performance of the three variants of SPAACE discussed in this paper are quantitatively evaluated within both grid-connected and isolated modes of operation of the DER based on the following metrics:

4.1.1. Computational Complexity

Computational complexity refers to the processing resources required for the execution of an algorithm. Computational complexity plays an important role in experimental validations due to the limited resources of RTTs and microcontrollers. This analysis presents the complexity of the different variants of the SPAACE algorithm with respect to the RTT utilized for its run and therefore is application- and scenario-agnostic. The following two key indicators are defined:

- Execution time: This refers to the time taken for the execution of SPAACE represented by T_{exec} .
- Memory requirement: This refers to the memory requirement of the algorithm as represented by M .

4.1.2. Dynamic Response

The performance of SPAACE is assessed for a change in the DER reference set point and by subjecting DER to a set of predefined common external disturbances based on the following key indicators:

- Settling time: The settling time T_{settling} is the time elapsed from the time of the disturbance to the time when the measured output signal $x(t)$ stays within the defined tolerance band ϵ .

$$T_{\text{settling}} = \operatorname{argmin}\{T_{\text{settling}} \in \mathcal{R} \mid \forall t > T_{\text{settling}} : x_{\text{band}}^+ < x(t) < x_{\text{band}}^-\} \quad (6)$$

- Overshoot: Defining the maximum excursion of $x(t)$ subject to an external disturbance or after a step change in the reference set point as x_{max} , the overshoot is calculated as

$$x_{\text{os}} = \left| \frac{x_{\text{max}} - x_{\text{sp}}}{x_{\text{sp}}} \right| \quad (7)$$

- Cumulative tracking error: Cumulative tracking error is defined as the sum of the tracking errors at every time step T_s from the application of the step or the disturbance to the time when the measured output signal has settled, i.e., T_{settling} .

$$S_e = \sum_{k=0}^N (x_{\text{sp}}[k] - x[k]) T_s \quad (8)$$

where $N = T_{\text{settling}}/T_s$. A smaller S_e corresponds to better set point tracking capability.

4.2. Computational Complexity Evaluation

The time and space complexity comparison of the three variants of SPAACE are presented in Figure 5 and Table 2 respectively. All implementations of SPAACE (linear, exponential, or quadratic) have a few common functions within and for the purpose of comparison only the mutually exclusive functions are considered. As can be observed from Figure 5, the linear predictor is computationally most efficient with an average $T_{\text{exec}} = 4.01 \mu\text{s}$, followed by quadratic with an average $T_{\text{exec}} = 4.95 \mu\text{s}$. The exponential predictor is computationally the most expensive with an average $T_{\text{exec}} = 185 \mu\text{s}$.

The space complexity is calculated in terms of the number of bits of storage required at a given point in time to allow for the prediction strategy to operate. The linear implementation requires only 32 bits (1 float value), followed by quadratic that requires 64 bits (2 float values) while the exponential prediction strategy has the highest space complexity requiring 320 bits (10 float values). The space complexity of linear and quadratic prediction strategies does not increase with larger prediction horizons for real-time implementation. On the other hand, the space complexity of exponential strategy increases linearly with the increase in the prediction horizon.

Table 2. Memory requirement comparison.

	Linear	Exponential	Quadratic
M	32	320	64

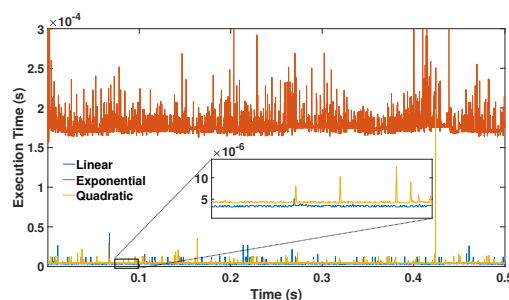


Figure 5. Execution time comparison.

4.3. Dynamic Response

4.3.1. Grid-Connected Operation

The DER dynamic response improvement is characterized subject to seven different events as summarized in Table 3. These events are chosen to be indicative of common scenarios in an inverter-dominated power system. The response of the DER subject to these seven events is presented in Figure 6a,b, where the former presents results when SPAACE is implemented within the DER while the latter where the SPAACE is implemented outwith the DER. The subfigures (a), (b), and (c) in both figures represent linear, exponential, and quadratic prediction strategy respectively. The results are further discussed below.

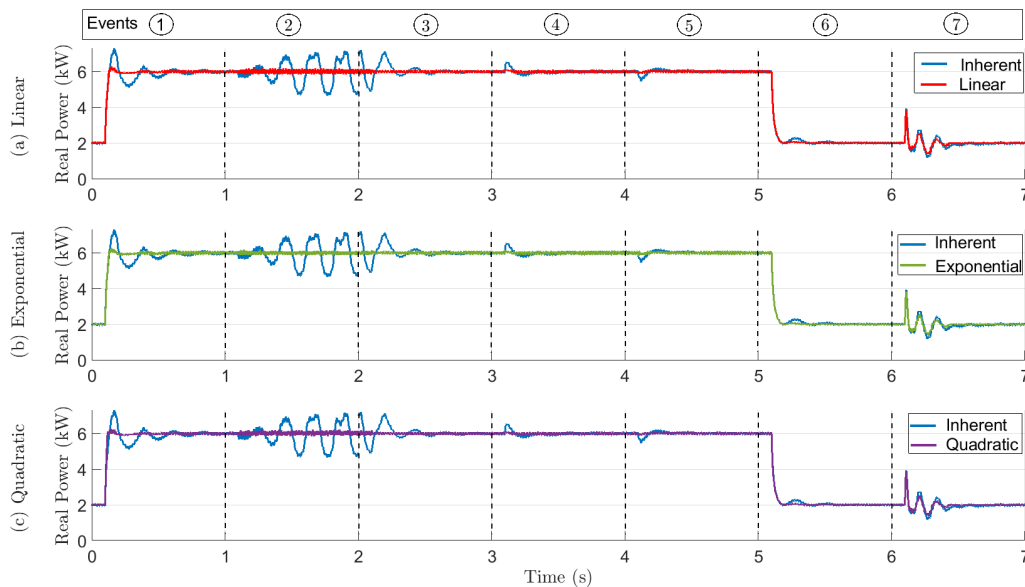
Table 3. Cases under consideration for the grid-connected operation

No.	Event	Change
1	Real power set point change	2 kW to 6 kW
2	Voltage change	1 pu to 1.1 pu
3	Voltage change	1.1 pu to 1 pu
4	Virtual impedance change	50 μ H to 5 μ H
5	Virtual impedance change	5 μ H to 50 μ H
6	Real power set point change	6 kW to 2 kW
7	Induction motor energization	7.5 kVA soft-start

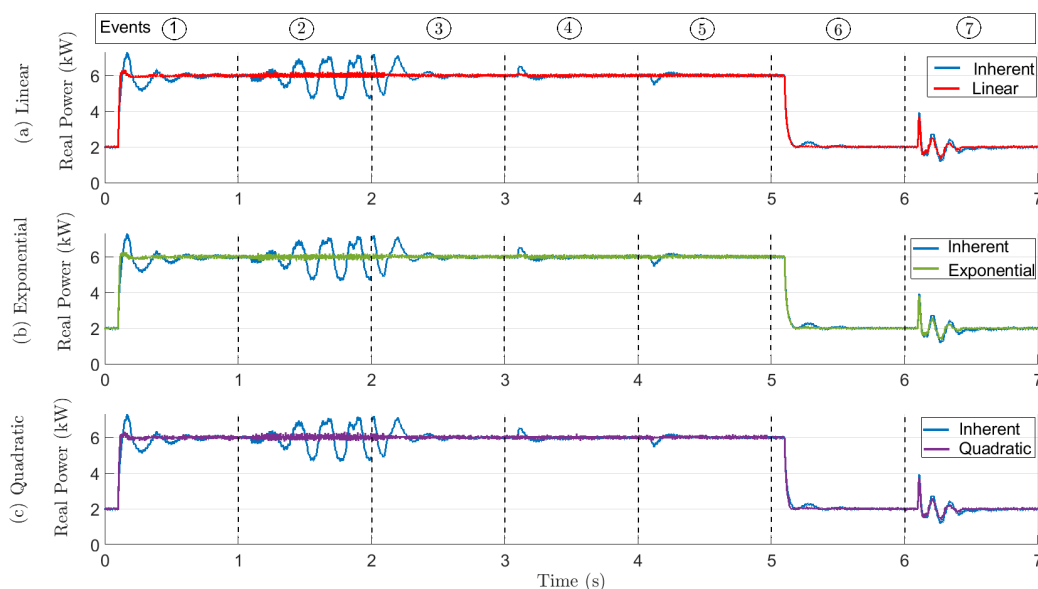
- (a) Set point change in real power: Events 1 and 6 emulate the day to day operations of a DER where, for example, the reference real power set point of a DER is changed based on its commitment to contribute to frequency control. The response of the DER subject to a real power set point change from 2 kW to 6 kW at $t = 0.1$ s and from 6 kW to 2 kW at $t = 5.1$ s is shown in columns 1 and 6 of Figure 6a,b with the performance indicators presented in Table 4. When SPAACE is incorporated, a minimum overshoot reduction of 16.52% for set point increase and 11.25% for set point decrease is observed. For step increase in set point, a minimum of 84.4% reduction in settling time is observed while for step decrease in set point the system response did not violate the tolerance band ϵ and therefore the settling time reported as 0 s.
- (b) Grid voltage set point change: Events 2 and 3 represent a set of transient conditions that can be expected within a distribution grid with high penetration of solar photovoltaic installations. A sudden cloud cover across a distribution feeder can lead to a drop in voltage, and the clearing of the cloud cover can lead to an increase in voltage. In this case study, the voltage magnitude is changed using the 90 kVA B2B module. The response of the DER subject to a grid voltage set point change from 1 pu to 1.1 pu at $t = 1.1$ s and from 1.1 pu to 1 pu at $t = 2.1$ s is shown in columns 2 and 3 of Figure 6a,b with the performance indicators presented in Table 4. The inherent controller employed for the grid-connected mode, in this case, works as a poorly tuned controller, for which the increase in system voltage causes oscillations in the power output. With SPAACE, the response of the system is well damped with improvement in overshoot observed.
- (c) Impact of system short-circuit ratio (SCR): Events 4 and 5 evaluate the dynamic performance of the DER subject to a change in system short circuit ratio (SCR). For 100% inverter-penetrated microgrids, changing the virtual impedance Z_v of individual inverters is an effective solution to improve overall system stability [61]. Changing Z_v of individual inverters in turn impacts the SCR of the system. The response of the DER to a change in virtual impedance is shown in columns 4 and 5 of Figure 6a,b, where Z_v is reduced from 50 μ H to 5 μ H at $t = 3.1$ s and increased back to 50 μ H at $t = 4.1$ s. The minimum improvement with SPAACE observed for overshoot reduction is 5.67%. With SPAACE, the response of the system does not violate the tolerance band ϵ , thus having a 0 s settling time.

Table 4. Dynamic response performance indicators for the seven events under the grid-connected mode for operation.

Event	Inherent			Linear			Exponential			Quadratic											
	Within DER			Within DER			Outwith DER			Within DER			Outwith DER								
	x_{os} (%)	T_s (s)	S_e $\times 10^6$	x_{os} (%)	T_s (s)	S_e $\times 10^6$	x_{os} (%)	T_s (s)	S_e $\times 10^6$	x_{os} (%)	T_s (s)	S_e $\times 10^6$	x_{os} (%)	T_s (s)	S_e $\times 10^6$	x_{os} (%)	T_s (s)	S_e $\times 10^6$			
1	21.75	0.44	2.34	4.72	0.07	0.55	5.23	0.06	0.42	4.13	0.05	0.59	4.36	0.06	0.49	4	0.06	0.38	5.1	0.07	0.46
2	18.95	-	5.34	2.72	-	0.22	3.63	-	0.28	2.87	-	0.08	3.52	-	0.28	3.03	-	0.25	5.25	-	0.47
3	15.64	0.34	2.01	0	0	0.02	0	0	0.06	0	0	0.06	0	0	0.13	0	0	0.03	0	0	0.14
4	8.72	0.18	0.43	2.06	0	0.01	2.57	0	0.04	2.2	0	0.09	3.32	0	0.18	2.15	0	0.01	3.33	0	0.09
5	9	0.17	0.36	1.93	0	0.06	1.37	0	0.15	2.96	0	0.06	2.97	0	0.15	1.83	0	0.01	3.33	0	0.1
6	16.2	0.22	0.91	4.95	0	0.66	1.8	0	0.63	4.45	0	0.65	2.5	0	0.63	4.65	0	0.64	2.3	0	0.5
7	96.75	0.33	1.53	91.9	0.31	0.9	84.55	0.246	0.89	91.15	0.25	0.94	90.85	0.25	0.96	91.1	0.25	0.92	86.95	0.25	0.93



(a) SPAACE implemented within the DER controller.



(b) SPAACE implemented outwith DER controller.

Figure 6. Dynamic response evaluation of SPAACE under grid connected mode of operation with.

(d) Induction motor energization: Event 7 evaluates the response of the DER subject to a switching transient on the network. For the system under study, the switching transient is emulated by

the energization of a 7.5 kVA induction motor. The response of the DER is shown in column 7 of Figure 6a,b. From the performance indicators presented in Table 4, it is evident that SPAACE improves the system performance with minimum overshoot reduction of 4.85% and a 7.4% reduction in settling time.

- (e) Cumulative tracking error: Table 4 also presents a comparison of the cumulative tracking error (S_e) for the inherent controller and the three variants of SPAACE under both implementations (within and outwith the DER). All variants of SPAACE reduce S_e for each of the seven events under consideration under both implementations. There is no distinctive performance difference between the three variants and the two implementations.
- (f) Summary: In this subsection, the dynamic performance of a weak controller operating in the grid-connected mode is evaluated. For the seven events under consideration, SPAACE considerably improves the dynamic performance with respect to each of the key indicators defined. This paper shows the feasibility of the implementation of SPAACE outwith the DER. In most cases, the performance of SPAACE when implemented outwith the DER is slightly inferior to its performance when it is implemented within the DER controller. This can be attributed to the communications delay to communicate the modified set point from the microcontroller to the DER internal controller. SPAACE's performance can be further optimized by considering the time delay during the design of the predictor.

4.3.2. Islanded Operation

The performance of SPAACE in the islanded mode of operation is evaluated for the DER subject to two events: (i) set point change in voltage from 1 pu to 0.9 pu at $t = 1.1$ s and (ii) increase in the real power of the load from 2 kW to 8 kW at $t = 2.1$ s. Figure 7 shows the DER response with SPAACE implemented outwith the controller, where subfigures (a), (b), and (c) represent linear, exponential, and quadratic prediction strategies, respectively. The performance indicators for islanded operation are summarised in Table 5.

Table 5. Dynamic response performance indicators for the two events under the islanded mode of operation.

Event	Inherent			Linear						Exponential						Quadratic					
	Within DER			Within DER			Outwith DER			Within DER			Outwith DER			Within DER			Outwith DER		
	x_{os} (%)	T_s (s)	S_e $\times 10^4$	x_{os} (%)	T_s (ms)	S_e $\times 10^4$	x_{os} (%)	T_s (ms)	S_e $\times 10^4$	x_{os} (%)	T_s (ms)	S_e $\times 10^4$	x_{os} (%)	T_s (ms)	S_e $\times 10^4$	x_{os} (%)	T_s (ms)	S_e $\times 10^4$	x_{os} (%)	T_s (ms)	S_e $\times 10^4$
1	0	2.81	0.05	0	1.75	0.02	0	1.81	0.03	0	1.76	0.03	0	1.81	0.03	0	1.75	0.03	0	1.82	0.04
2	0	0	3.24	0	0	3.22	0	0	3.24	0	0	3.23	0	0	3.23	0	0	3.23	0	0	3.24

The DER controller utilized for islanded operation typically needs to be well-tuned and robust to be able to maintain the voltage under varied load conditions. As can be observed, although the inherent controller does not present any overshoot for a change in voltage set point, SPAACE still does improve the speed of its response. The increase in load causes a transient in voltage that is well mitigated by the inherent controller; SPAACE brings the system to the steady-state even faster. This behavior is corroborated by the cumulative tracking error S_e presented in Table 5, where reduced S_e for event 1 corresponds to the increase in response speed. No significant difference in performance under a step increase in load is observed.

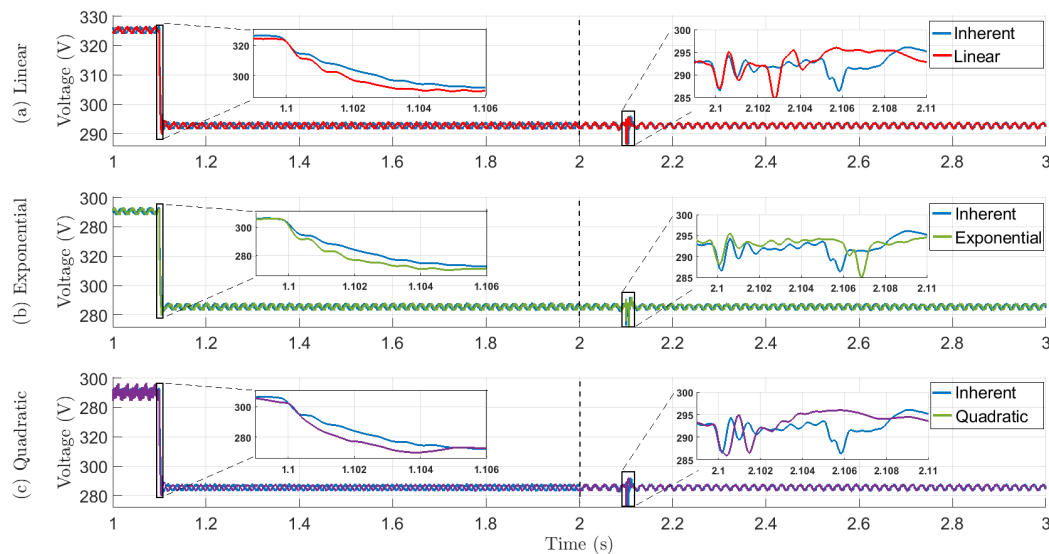


Figure 7. Dynamic response evaluation of SPAACE under the islanded mode of operation. SPAACE is implemented outwith the DER controller.

5. Conclusions

In this paper, a high-fidelity hardware-in-the-loop experimental test bed has been utilized to prove the practical real-world feasibility of an add-on controller, SPAACE, designed to improve the performance of existing controllers in an inverter-dominated power system. Following a methodological approach, first, an application- and scenario-agnostic computational performance evaluation of three prediction strategies for SPAACE is undertaken; followed by an application-oriented dynamic performance evaluation. With the defined computational and dynamic performance metrics, the following observations are highlighted:

- The linear predictor is computationally the most efficient with the least time and space complexity. In addition, the time and space complexity of a linear predictor does not increase with an increase in the prediction horizon.
- The choice of predictor only marginally impacts the dynamic performance and therefore, based on the computational performance evaluation, the use of a linear predictor is recommended. This is an application-specific recommendation, however, the trade-off between computational and dynamic performance should be assessed, specifically given the demonstrated close performance of linear and quadratic predictors.
- With a weak controller (in grid-connected mode), the incorporation of SPAACE leads to improvement in the dynamic properties (at least one of settling time, overshoot, and tracking error) of the response subject to the studied disturbances. With a strong controller (in islanded mode), the impact of SPAACE is limited to bringing the system to steady-state faster.
- The set of events chosen are non-exhaustive but sufficient for demonstration of the performance of the approach under a broad range of circumstances. However, given the versatility of its operation, the improvement of dynamics under unknown system conditions can be expected.

Furthermore, in this paper, SPAACE's implementation external to a primary controller has been demonstrated. A slight deterioration in the performance of SPAACE compared to its implementation within the primary controller is observed. This deterioration in performance is associated with the time delay of the implementation that highlights an important aspect of future work, i.e., to incorporate time delay within the design of the predictor.

The requirement for incorporation of SPAACE is the existing capability DER controller to accept external setpoints (implementation outwith DER) or access to the internal control (implementation

within DER). However, this does not present as a limitation as without either one of the above requirements, the DER would not be able to participate within ancillary services provision.

Author Contributions: Conceptualization, M.H.S. and A.M.-S.; funding acquisition, A.M.-S. and G.M.B.; methodology, M.H.S. and A.M.-S.; validation, M.H.S. and E.G.-S.; writing—original draft, M.H.S. and A.M.-S.; writing—review and editing, E.G.-S. and G.M.B. All authors have read and agreed to the published version of the manuscript.

Funding: This work was supported in part by the European Commission under the H2020 Programme’s ERIGRID and ERIGRID2.0 projects (grant no: 654113 and 870620) and in part by the U.S. National Science Foundation under grants EPCN-1509895 and CPS-1837700. Any opinions, findings, and conclusions or recommendations expressed in this material are those of the authors and do not necessarily reflect those of the funding bodies.

Conflicts of Interest: The authors declare no conflict of interest.

Nomenclature

Abbreviations

SPAACE	Set point automatic adjustment with correction enabled.
SPM	Set point modulation.
DER	Distributed energy resource.
HIL	Hardware-in-the-loop.
SISO	Single input single output.
LSE	Least square error.
DPSSL	Dynamic power systems laboratory.
B2B	Back to back.
RTT	Real time target.
SCR	Short circuit ratio.
HVDC	High voltage direct current.
BESS	Battery energy storage system.
DRTS	Digital real-time simulator.

Variables

x_{sp}	Reference set point.
x	Measured output.
x_1	Initial reference set point.
x_2	Final reference set point.
x'_{sp}	Modified set point.
m	Scaling factor.
T_{pred}	Horizon of prediction.
n	An integer value.
\hat{x}	Predicted value of x .
r	Average rate of change of historical data.
q	Second derivative of historical data.
P_{sp}	Real power set point.
Q_{sp}	Reactive power set point.
P_{meas}	Measured real power.
Q_{meas}	Measured reactive power.
P'_{sp}	Modified real power set point.
Q'_{sp}	Modified reactive power set point.
V_{dq}	Direct and quadrature components of voltage.
I_{dq}	Direct and quadrature components of current.
V_{sp}	Voltage set point.
f_{sp}	Frequency set point.
V_{meas}	Measured voltage.
f_{meas}	Measured frequency.
V'_{sp}	Modified voltage set point.

f'_{sp}	Modified frequency set point.
S_{1-6}	Switches within the utilized network.
$L_{1-2,v}$	Line impedances within the utilized network.
T_{exec}	Execution time.
M	Memory requirement.
$T_{settling}$	Settling time.
x_{max}	Absolute maximum value of x .
T_s	Time step.
S_e	Cumulative tracking error.
x_{os}	Overshoot.
Z_v	Virtual impedance.
T_{past}	Window of prediction history.
x_{band}^+	Upper threshold of tolerance band.
x_{band}^-	Lower threshold of tolerance band.
ϵ	Tolerance band.
ω_0	Dominant natural frequency.

References

1. Fan, B.; Peng, J.; Yang, Q.; Liu, W. Distributed Periodic Event-Triggered Algorithm for Current Sharing and Voltage Regulation in DC Microgrids. *IEEE Trans. Smart Grid* **2020**, *11*, 577–589. [[CrossRef](#)]
2. Fan, B.; Guo, S.; Peng, J.; Yang, Q.; Liu, W.; Liu, L. A Consensus-Based Algorithm for Power Sharing and Voltage Regulation in DC Microgrids. *IEEE Trans. Ind. Inform.* **2020**, *16*, 3987–3996. [[CrossRef](#)]
3. Ding, D.; Han, Q.-L.; Wang, Z.; Ge, X. A Survey on Model-Based Distributed Control and Filtering for Industrial Cyber-Physical Systems. *IEEE Trans. Ind. Inform.* **2019**, *15*, 2483–2499. [[CrossRef](#)]
4. Molzahn, D.K.; Dorfler, F.; Sandberg, H.; Low, S.H.; Chakrabarti, S.; Baldick, R.; Lavaei, J. A Survey of Distributed Optimization and Control Algorithms for Electric Power Systems. *IEEE Trans. Smart Grid* **2017**, *8*, 2941–2962. [[CrossRef](#)]
5. Li, H.; Li, F.; Xu, Y.; Rizy, D.T.; Kueck, J.D. Adaptive Voltage Control With Distributed Energy Resources: Algorithm, Theoretical Analysis, Simulation, and Field Test Verification. *IEEE Trans. Power Syst.* **2010**, *25*, 1638–1647. [[CrossRef](#)]
6. Leithead, W. Survey of Gain-Scheduling Analysis Design. *Int. J. Control* **1999**, *73*, 1001–1025. [[CrossRef](#)]
7. Namara, P.M.; Negenborn, R.R.; Schutter, B.D.; Lightbody, G. Optimal Coordination of a Multiple HVDC Link System Using Centralized and Distributed Control. *IEEE Trans. Control Syst. Technol.* **2013**, *21*, 302–314. [[CrossRef](#)]
8. Moradzadeh, M.; Boel, R.; Vandeveld, L. Voltage Coordination in Multi-Area Power Systems via Distributed Model Predictive Control. *IEEE Trans. Power Syst.* **2013**, *28*, 513–521. [[CrossRef](#)]
9. Roshany-Yamchi, S.; Cychowski, M.; Negenborn, R.; Schutter, B.; Delaney, K.; Connell, J. Kalman Filter-Based Distributed Predictive Control of Large-Scale Multi-Rate Systems: Application to Power Networks. *IEEE Trans. Control. Syst. Technol.* **2013**, *21*, 27–39. [[CrossRef](#)]
10. Liu, X.; Kong, X.; Lee, K.Y. Distributed model predictive control for load frequency control with dynamic fuzzy valve position modelling for hydro-thermal power system. *IET Control Theory Appl.* **2016**, *10*, 1653–1664. [[CrossRef](#)]
11. Mehmood, F.; Khan, B.; Ali, S.M.; Rossiter, J.A. Distributed model predictive based secondary control for economic production and frequency regulation of MG. *IET Control Theory Appl.* **2019**, *13*, 2948–2958. [[CrossRef](#)]
12. Åström, K.J.; Häggglund, T. *PID Controllers: Theory, Design and Tuning*, 2nd ed.; Instrument society of America: Research Triangle Park, NC, USA, 1995.
13. Åström, K.J. Auto-Tuning, Adaptation and Expert Control. In Proceedings of the American Control Conference, Boston, MA, USA, 19–21 June 1985; pp. 1514–1519.
14. Åström, K.J.; Murray, R.M. *Feedback Systems: An Introduction for Scientists and Engineers*, 2nd ed.; Princeton University Press: Princeton, NJ, USA, 2008.
15. Åström, K.J.; Häggglund, T. Automatic Tuning of PID Controllers. In *The Control Handbook*; Levin, W., Ed.; Number 53; CRC Press: Boca Raton, FL, USA, 1996.

16. Killingsworth, N.; Krstic, M. PID Tuning Using Extremum Seeking: Online, model-free performance optimization. *IEEE Control Syst. Mag.* **2006**, *26*, 70–79.
17. Hjalmarsson, H.; Gevers, M.; Gunnarsson, S.; Lequin, O. Iterative feedback tuning: Theory and applications. *IEEE Control. Syst.* **1998**, *18*, 26–41.
18. Lequin, O.; Bosmans, E.; Triest, T. Iterative feedback tuning of PID parameters: Comparison with classical tuning rules. *Contr. Eng. Pract.* **2003**, *11*, 1023–1033. [[CrossRef](#)]
19. Lequin, O.; Gevers, M.; Triest, T. Optimizing the settling time with iterative feedback tuning. In Proceedings of the 15th IFAC World Congress, Beijing, China, 5–9 July 1999; pp. 433–437.
20. Burns, D.J.; Laughman, C.R.; Guay, M. Proportional–Integral Extremum Seeking for Vapor Compression Systems. *IEEE Trans. Control Syst. Technol.* **2020**, *28*, 403–412. [[CrossRef](#)]
21. Hunnekens, B.; Dino, A.D.; van de Wouw, N.; van Dijk, N.; Nijmeijer, H. Extremum-Seeking Control for the Adaptive Design of Variable Gain Controllers. *IEEE Trans. Control Syst. Technol.* **2015**, *23*, 1041–1051. [[CrossRef](#)]
22. Lu, X.; Krstić, M.; Chai, T.; Fu, J. Hardware-in-the-Loop Multiobjective Extremum-Seeking Control of Mineral Grinding. *IEEE Trans. Control Syst. Technol.* **2020**, 1–11. [[CrossRef](#)]
23. Smith, O.J.M. Posicast Control of Damped Oscillatory Systems. *Proc. IRE* **1957**, *45*, 1249–1255. [[CrossRef](#)]
24. Hung, J.Y. Feedback Control with Posicast. *IEEE Trans. Ind. Electron.* **2003**, *50*, 94–99. [[CrossRef](#)]
25. Vaughan, J.; Smith, A.; Kang, S.J.; Singhose, W. Predictive Graphical User Interface Elements to Improve Crane Operator Performance. *IEEE Trans. Syst. Man Cybern. Part A Syst. Hum.* **2011**, *41*, 323–330. [[CrossRef](#)]
26. Cook, G. An Application of Half-Cycle Posicast. *IEEE Trans. Autom. Control* **1966**, *11*, 556–559. [[CrossRef](#)]
27. Hung, J.Y. Posicast Control Past and Present. *IEEE Multidiscip. Eng. Educ. Mag.* **2007**, *2*, 7–11.
28. Feng, Q.; Nelms, R.M.; Hung, J.Y. Posicast-Based Digital Control of the Buck Converter. *IEEE Trans. Ind. Electron.* **2006**, *53*, 759–767. [[CrossRef](#)]
29. Mi, Y.; Song, Y.; Fu, Y.; Wang, C. The Adaptive Sliding Mode Reactive Power Control Strategy for Isolated Wind-Diesel Power System Based on Sliding Mode Observer. *IEEE Trans. Sustain. Energy* **2019**. [[CrossRef](#)]
30. Zhang, Y.; Li, G. Non-causal Linear Optimal Control of Wave Energy Converters with Enhanced Robustness by Sliding Mode Control. *IEEE Trans. Sustain. Energy* **2019**. [[CrossRef](#)]
31. Onyeka, A.E.; Xing-Gang, Y.; Mao, Z.; Jiang, B.; Zhang, Q.; Yan, X. Robust decentralised load frequency control for interconnected time delay power systems using sliding mode techniques. *IET Control Theory Appl.* **2020**, *14*, 470–480. [[CrossRef](#)]
32. Sarkar, M.K.; Dev, A.; Asthana, P.; Narzary, D. Chattering free robust adaptive integral higher order sliding mode control for load frequency problems in multi-area power systems. *IET Control Theory Appl.* **2018**, *12*, 1216–1227. [[CrossRef](#)]
33. Zhang, H.; Zhou, J.; Sun, Q.; Guerrero, J.M.; Ma, D. Data-Driven Control for Interlinked AC/DC Microgrids Via Model-Free Adaptive Control and Dual-Droop Control. *IEEE Trans. Smart Grid* **2017**, *8*, 557–571. [[CrossRef](#)]
34. Safaei, A.; Mahyuddin, M.N. Adaptive Model-Free Control Based on an Ultra-Local Model With Model-Free Parameter Estimations for a Generic SISO System. *IEEE Access* **2018**, *6*, 4266–4275. [[CrossRef](#)]
35. Hou, Z.; Zhu, Y. Controller-Dynamic-Linearization-Based Model Free Adaptive Control for Discrete-Time Nonlinear Systems. *IEEE Trans. Ind. Inform.* **2013**, *9*, 2301–2309. [[CrossRef](#)]
36. Chen, J.; Yang, F.; Han, Q.-L. Model-Free Predictive H_∞ Control for Grid-Connected Solar Power Generation Systems. *IEEE Trans. Control Syst. Technol.* **2014**, *22*, 2039–2047. [[CrossRef](#)]
37. Duan, L.; Hou, Z.; Yu, X.; Jin, S.; Lu, K. Data-Driven Model-Free Adaptive Attitude Control Approach for Launch Vehicle With Virtual Reference Feedback Parameters Tuning Method. *IEEE Access* **2019**, *7*, 54106–54116. [[CrossRef](#)]
38. Lu, C.; Zhao, Y.; Men, K.; Tu, L.; Han, Y. Wide-area power system stabiliser based on model-free adaptive control. *IET Control Theory Appl.* **2015**, *9*, 1996–2007. [[CrossRef](#)]
39. Wang, H.; Yang, J.; Chen, Z.; Ge, W.; Li, Y.; Ma, Y.; Dong, J.; Okoye, M.O.; Yang, L.; Onyeka, O.M. Analysis and Suppression for Frequency Oscillation in a Wind-Diesel System. *IEEE Access* **2019**, *7*, 22818–22828. [[CrossRef](#)]
40. Zolfaghari, M.; Hosseini, S.H.; Fathi, S.H.; Abedi, M.; Gharehpetian, G.B.; Fathi, S.H. A New Power Management Scheme for Parallel-Connected PV Systems in Microgrids. *IEEE Trans. Sustain. Energy* **2018**, *9*, 1605–1617. [[CrossRef](#)]

41. M'Zoughi, F.; Garrido, I.; Garrido, A.J.; De La Sen, M. Fuzzy Gain Scheduled-Sliding Mode Rotational Speed Control of an Oscillating Water Column. *IEEE Access* **2020**, *8*, 45853–45873. [[CrossRef](#)]
42. Sun, H.; Zong, G.; Ahn, C.K. Quantized Decentralized Adaptive Neural Network PI Tracking Control for Uncertain Interconnected Nonlinear Systems With Dynamic Uncertainties. *IEEE Trans. Syst. Man Cybern. Syst.* **2019**, 1–14. [[CrossRef](#)]
43. Su, X.; Liu, Z.; Zhang, Y.; Chen, C.L.P. Event-Triggered Adaptive Fuzzy Tracking Control for Uncertain Nonlinear Systems Preceded by Unknown Prandtl-Ishlinskii Hysteresis. *IEEE Trans. Cybern.* **2019**, 1–14. [[CrossRef](#)]
44. Mehrizi-Sani, A.; Iravani, R. Online Set Point Adjustment for Trajectory Shaping in Microgrid Applications. *IEEE Trans. Power Syst.* **2012**, *27*, 216–223. [[CrossRef](#)]
45. Yazdani, M.; Mehrizi-Sani, A.; Seebacher, R.; Krischan, K.; Muetze, A. Smooth reference modulation to improve dynamic response in drive systems. *IEEE Trans. Power Electron.* **2018**, *33*, 6434–6443. [[CrossRef](#)]
46. Mehrizi-Sani, A.; Iravani, R. Online Set Point Modulation to Enhance Microgrid Dynamic Response: Theoretical Foundation. *IEEE Trans. Power Syst.* **2012**, *27*, 2167–2174. [[CrossRef](#)]
47. Ghaffarzadeh, H.; Stone, C.; Mehrizi-Sani, A. Predictive set point modulation to mitigate transients in lightly damped balanced and unbalanced systems. *IEEE Trans. Power Syst.* **2016**, *32*, 1041–1049. [[CrossRef](#)]
48. Ghaffarzadeh, H.; Mehrizi-Sani, A. Predictive set point modulation to mitigate transients in power systems with a multiple-input-multiple-output control system. In Proceedings of the IEEE Innovative Smart Grid Technologies Conference (ISGT), Minneapolis, MN, USA, 6–9 September 2016.
49. Mehrizi-Sani, A.; Iravani, R. Performance Evaluation of a Distributed Control Scheme for Overvoltage Mitigation. In Proceedings of the CIGRÉ International Symposium on The Electric Power System of The Future: Integrating supergrids and microgrids, Bologna, Italy, 13–15 September 2011.
50. Sandia National Laboratories. *Test Protocols for Advances Inverter Interoperability Functions*; Sandia Corporation: Albuquerque, NM, USA, 2013; pp. 1–22.
51. Guillo-Sansano, E.; Syed, M.H.; Roscoe, A.J.; Burt, G.M. Initialization and Synchronization of Power Hardware-In-The-Loop Simulations: A Great Britain Network Case Study. *Energies* **2018**, *11*, 1087. [[CrossRef](#)]
52. Guillo-Sansano, E.; Syed, M.H.; Roscoe, A.J.; Burt, G.M.; Coffele, F. Characterization of Time Delay in Power Hardware in the Loop Setups. *IEEE Trans. Ind. Electron.* **2020**, *50*, 1–10. [[CrossRef](#)]
53. Blair, S.M.; Syed, M.H.; Roscoe, A.J.; Burt, G.M.; Braun, J. Measurement and Analysis of PMU Reporting Latency for Smart Grid Protection and Control Applications. *IEEE Access* **2019**, *7*, 48689–48698. [[CrossRef](#)]
54. Guillo-Sansano, E.; Roscoe, A.J.; Burt, G.M. Harmonic-by-harmonic time delay compensation method for PHIL simulation of low impedance power systems. In Proceedings of the 2015 International Symposium on Smart Electric Distribution Systems and Technologies (EDST), Vienna, Austria, 8–11 September 2015; pp. 560–565. [[CrossRef](#)]
55. Li, Q.; Yu, S.; Al-Sumaiti, A.; Turitsyn, K. Modeling and Co-Optimization of a Micro Water-Energy Nexus for Smart Communities. In Proceedings of the 2018 IEEE PES Innovative Smart Grid Technologies Conference Europe (ISGT-Europe), Sarajevo, Bosnia-Herzegovina, 21–25 October 2018; pp. 1–5.
56. Hao, H.; Somani, A.; Lian, J.; Carroll, T.E. Generalized aggregation and coordination of residential loads in a smart community. In Proceedings of the 2015 IEEE International Conference on Smart Grid Communications (SmartGridComm), Miami, FL, USA, 2–5 november 2015; pp. 67–72.
57. Syed, M.H.; Guillo-Sansano, E.; Avras, A.; Downie, A.; Jennett, K.; Burt, G.M.; Coffele, F.; Rudd, A.; Bright, C. The Role of Experimental Test Beds for the Systems Testing of Future Marine Electrical Power Systems. In Proceedings of the 2019 IEEE Electric Ship Technologies Symposium (ESTS), Washington, DC, USA, 14–16 August 2019; pp. 141–148.
58. Kontis, E.O.; Nousedilis, A.I.; Papagiannis, G.K.; Syed, M.H.; Guillo-Sansano, E.; Burt, G.; Papadopoulos, T.A. Power Hardware-in-the-Loop Setup for Developing, Analyzing and Testing Mode Identification Techniques and Dynamic Equivalent Models. In Proceedings of the 2019 IEEE Milan PowerTech, Milan, Italy, 23–27 June 2019; pp. 1–6.
59. Syed, M.H.; Sansano, E.G.; Blair, S.M.; Burt, G.; Prostejovsky, A.M.; Rikos, E. Enhanced load frequency control: Incorporating locational information for temporal enhancement. *IET Gener. Transm. Distrib.* **2019**, *13*, 1865–1874. [[CrossRef](#)]

60. Wang, Y.; Syed, M.H.; Guillo-Sansano, E.; Xu, Y.; Burt, G.M. Inverter-Based Voltage Control of Distribution Networks: A Three-Level Coordinated Method and Power Hardware-in-the-Loop Validation. *IEEE Trans. Sustain. Energy* **2019**. [[CrossRef](#)]
61. Lu, X.; Sun, K.; Guerrero, J.M.; Vasquez, J.C.; Huang, L.; Wang, J. Stability Enhancement Based on Virtual Impedance for DC Microgrids With Constant Power Loads. *IEEE Trans. Smart Grid* **2015**, *6*, 2770–2783. [[CrossRef](#)]



© 2020 by the authors. Licensee MDPI, Basel, Switzerland. This article is an open access article distributed under the terms and conditions of the Creative Commons Attribution (CC BY) license (<http://creativecommons.org/licenses/by/4.0/>).

© 2020. This work is licensed under <http://creativecommons.org/licenses/by/3.0/> (the “License”). Notwithstanding the ProQuest Terms and Conditions, you may use this content in accordance with the terms of the License.